Manuscript Details

Manuscript number	JMIC_2017_319_R1
Title	Specimen Preparation for Nano-scale Investigation of Cementitious Repair Material (CRM)
Article type	Full Length Article

Abstract

Cementitious Repair Materials (CRMs) in the construction industry have been used for many decades now and has become a very important part of activities in cement world. The performance of some of these CRMs when applied to retrofitting concrete structural elements is also well documented. However, the characterization of some of the CRMs at the micro- and nano level is not fully documented. The first step to studying materials at the microscopic level is to be able to fabricate proper specimens for microscopy. In this study, a special and newly developed class of CRM was selected and fabricated by Focused Ion Beam (FIB) using well-known “Lift-out” technique. The prepared specimen was later examined using various analytical techniques such as energy dispersive x-ray analysis using one of the highest and most stable Scanning Transmission Electron Holography Microscopy (STEHM) around the world. This process enabled understanding of the composition, morphology, and spatial distribution of various phases of the CRM. It was observed that the micro-structure consisted of a very fine, compact, and homogeneous amorphous structure. X-ray analysis indicated that there was considerable deviation between the Si/Ca ratios for the hydrated product.

Keywords	Specimen Preparation, Focused Ion Beam, Cementitious Materials, Scanning Transmission Electron Holography Microscopy (STEHM), Electron Diffraction Pattern
Manuscript category	Ray Egerton - Physical Science

Corresponding Author	pejman azarsa
Corresponding Author's Institution	university of victoria
Order of Authors	pejman azarsa, Rishi Gupta

Suggested reviewers	Meghdad Hoseini, Ahmed Sharif, Aali Alizadeh, ali akbar Ramezanianpour

Submission Files Included in this PDF

File Name [File Type]

Cover letter.docx [Cover Letter]

Reviewer comments (Micron Journal)_Azarsa_Gupta.docx [Response to Reviewers]

Highlights.docx [Highlights]

Revised_Specimen Prep for Nano-scale Investigation of CRM_PA.docx [Manuscript File]

To view all the submission files, including those not included in the PDF, click on the manuscript title on your EVISE Homepage, then click 'Download zip file'.

Department of Civil Engineering
Faculty of Engineering
Engineering Computer Science (ECS), Room 304
PO Box 1700, Victoria, BC V8W 2Y2
Telephone: 250-472-5840| Fax: 250-721-6051
email: pazarsa@uvic.ca

October 30, 2017

Drs. Filip Braet and Ray Egerton
Editor-in-Chief
Micron Journal

Subject: submission of journal article

Dear Drs. Braet and Egerton,

Please find included in this submission a paper entitled "**Specimen Preparation for Nano-scale Investigation of Cementitious Repair Material."**

This paper is being submitted for your consideration for publication in the Micron Journal. The coauthor of this paper is Dr. Rishi Gupta from University of Victoria. The paper highlights the much-needed research in the nano-scale investigation of cement-based repair materials and also presents step by step procedure to prepare appropriate size specimen using Focused Ion Beam (FIB) system for examination of newly developed concrete repair material under Scanning Transmission Electron Holography Microscopy (STEHM). This study is expected to be of significant value in the investigation of the repair materials' nanostructure and the composition of hydration product, and thus may provide a valuable tool in understanding and further development of these construction materials.

Please feel free to contact me if you have any questions or comments.

Regards,

Pejman Azarsa

Specimen Preparation for Nano-scale Investigation of Cementitious Repair Material

Authors: Pejman Azarsa, Rishi Gupta January 2018

Editor

No.	Comments	Response
1	I can accept the revised manuscript for publication in Micron if you will kindly change the reference style to that required by the journal, which is of the form: (Smith, 2000; Jones et al., 1995) within the text and an alphabetical (by first author surname) list at the end, including the TITLE and PAGE RANGE of each article.	All references within text as well as the list at the end were modified to the journal reference style.

Reviewer 1

No.	Comments	Response
1	The overall contribution of this manuscript is much less than its length. The authors should more focus on STEHM study. The authors should delete some of the details of some characterization techniques.	The authors thank the reviewer for the detailed review provided on the paper with very valuable comments. To reduce the manuscript length and keep the focus on STEHM study while not to mention the details of some characterization techniques, the following modifications have been done in the text: • Figure 4 was removed. • Details of the characterization technique have been removed: "*The characteristic X-ray typically used in EDS are created when high-energy electrons of the beam eject inner shell electrons from atoms in the sample, and the ionized atoms return to their lowest energy states by replacing the missing inner shell electrons by electrons from the outer shells. This process results in either the emission of an X-ray or an Auger electron, whose energy of emission is characteristic of the difference in energy of the two electron shells involved, thereby providing a unique signature to identify the type of atoms present. In a EDS spectrum, sharp peaks related to the characteristic X-ray emitted by the atoms of the different elements present in the sample."* • Figure 7 was removed. • Details of the characterization technique have been removed: *"λ is a function of the beam energy and of the specimen thickness."* • Details of the characterization technique have been removed: *"An electron will typically undergo repeated energy losses upon traversing the sample. The scattering follows Poisson statistics, so the probability of n-fold scattering is (Ghosh et al., 2015):*

		$P_n = \frac{\left(\frac{t}{\lambda}\right)_n exp\left(-{}^{t}/_{\lambda}\right)}{n!}$ *and probability of no-scattering,* $P_0 = exp\left(-{}^{t}/_{\lambda}\right) = {}^{I_0}/_{I_t}$. *Therefore, thickness,* $t = \lambda \times ln\left({}^{I_0}/_{I_t}\right)$, *where* $I_t =$ *total spectrum integral,* $I_0 =$ *zero-loss peak integral. The "Thickness Map" provides the relative thickness (*${}^{t}/_{\lambda}$*) map of a specimen in the form of an image based on the above formula."* • Details of the characterization technique have been removed: *"To view the diffraction pattern from a specimen, the imaging-system lenses of the microscope were adjusted such that the back focal plane of the objective lenses act as the object plane for the intermediate lenses. This causes the diffraction pattern to be projected onto the viewing screen."*
2	Authors should give chemical composition of the CRM as it is available. It is important to know the amount of polymeric materials if any. Individual particles like **$(CaO)_3$. Al_2O_3, $(CaO)_2$. SiO_2, $(CaO)_3$.SiO_2** are present or not. The presence of **Mg** is noticeable, then its chemical nature is also important.	This comment has been addressed. As mentioned in the text, the chemical compositions of this product are proprietary and not available, however authors added some details in the text to provide a wider insight about this product. **"This is referred to as a modified synthetic CRM which contains Portland cement, reactive silica, calcium and aluminum salts of organic acids and bases, and some crystalline catalysts (Kumar et al., 2009)."** Also, authors referenced two published articles in the text that describe the chemical compositions and IR spectra of similar product. **"The chemical compositions and IR spectra of similar product have been reported in (Kumar et al., 2009; Sisomphon et al., 2012)."** To keep the focus of the paper on the characterisation techniques using sub-micron images, authors added at various places within the text what would be useful for the readers to know. These details include details of EDS analysis, but the focus has only been on conceivable techniques to visualize the x-ray analysis data and how to obtain information about hydration products and not to draw any conclusions about the CRM materials. Also, in the paper the usefulness of the x-ray analysis to find proper specimens prior to micro fabrication using FIB

		and later for STEHM study is included. Here are examples of what have been added in the revised text. **"As one of the preparation steps, the x-ray analysis has only been done to select proper location for thinning procedure as well as STEHM investigation and not to draw any conclusions about CRM chemical compositions."** **"Although more sampling from the CRM and its chemical compositions are needed for comprehensive conclusions, the plot of Si/Ca vs Al/Ca in Figure 6-(a) shows that calcium hydroxide ($Ca(OH)_2$) was the main product of selected regions in 7-days hydrated CRM."** **"However, the goal of this work was to establish an experimental methodology as opposed to determining the absolute proportions of various elements."** **"Moreover, EDS analyses for un- and hydrated CRM for 7-days are plotted as atomic percentage, another way of data representation, normalized to 100%, in Ca-Si-(Al+Mg) ternary diagram in Figure 7."** **"Generally, preliminary experiments have shown that determination of specimen's composition by EDS combined with STEHM is feasible, however, the variability of Ca and Si was too severe to allow fully quantitative results to be presented from these initial experiments."**
3	The particles size is 40-150 µm, however, from Fig. 1 it seems more than 1 mm.	Authors agree with the reviewer and modified the text as follows: **"Although the anhydrous particles' size reported by its supplier is about 40-150 µm, it should be noted that the particles' size measured from SEM images turned out to be above 20 µm and less than 1.5 mm. Hence, picking a suitable particle size for thinning procedure was quite a challenging task."**
4	The author should provide a simple XRD study of the hydrated CRM as an evidence of noncrystalinity from the STEHM study.	As a well-known reliable characterization technique, authors used SAED patterns from STEHM to obtain crystallographical information and determine whether the observed CRM particle has crystalline or amorphous structure. At this point, authors are not able to conduct XRD study to identify nanocrystalinity of CRM particle due to lack of available resources. In any case, the authors are in agreement with the reviewer and have added the following text: **"As an additional characterization technique, a simple XRD examination can be also performed to**

		identify non-crystalinity of the hydrated CRM particle."
5	The presence of Ga makes the EDS of TEM less interesting.	Authors agree with the reviewer completely. The possible sources of specimen's damage have been discussed in the paper. An operator should also be aware that contamination from electron beam may occur during imaging. To provide more clarity on this, the following sentence is now included in the text: **"Evidence of Gallium (Ga), most likely sputtered from electron beam, was also observed in different spots which cautiously needs to be prevented during sample preparation as it makes EDS analysis of investigated sample less appealing."**
6	The most important thing is the sampling of CRM for TEM study. It would be wonderful to have several TEM samples from hydrous CRM compact for fact finding.	Authors agree with the reviewer's point about need of more samples to draw more precise conclusions; however, the specimen was divided into five different regions to increase the reliability of the proposed method. Also, the STEHM microscope used in this study is one of the most stable and high-resolution microscopes in the world which provides reliable results and best quality images, but the cost and resources associated with microscope are quite high and as such preparation of more samples needs more funding resources which was not available to the authors. Authors believe the proposed experimental methodology itself, is a quite novel and well-documented technique that will add enough value to current state of knowledge in the study of cement-based materials. Authors are in agreement with the reviewer and hence the following sentences were also added to the text: **"It should be noted that even though one sample was mounted on the stub, the sample was divided into five areas, thus increasing the reliability of the results."** **"Overall, the safe statement that can be made at this point is that SAED patterns of observed CRM particle show amorphous structure; however, more samples are required to be prepared for a comprehensive conclusion."**

Reviewer 2

No.	Comments	Response
1	How do you think the presence of minerals in tap water could affect the formation of hydration products? In addition, the presence of carbon dioxide in tap water as well as the carbon dioxide from air can result in the carbonation of the hydration products? How did you eliminate this? (In general,	The authors appreciate the time taken by the reviewer in providing very valuable comments. Since the focus of this study is to fabricate specimen in compliance with: (i) concrete construction standards such as ASTM and CSA, (ii) according to the supplier recommendations, and (iii) considering practical real-world situation, tap (potable) water was used. Authors

	one of the critical steps in the preparation of relatively small specimens for nano-scale surface-based studies in cement-based hydrates is to eliminate the risk of carbonation when handling the specimens in the ambient conditions. Any slight exposure to carbon dioxide in the air could results in the surface carbonation in the cement-based hydration products and affect the results of experiments dealing with surface properties. This level of carbonation may not necessarily be detected by methods such as TGA or XRD as they deal with bulk properties).	have included the following sentences in the text to incorporate the reviewer's comment to address possible effects of using tap water instead of distilled (pure) water. **"It is reported that there can be some negative effects of using tap water instead of distilled water. Negative effects reported include: decrease in initial and final setting time mainly due to flocculation process on setting and reduction in pH level of the paste due to presence of bicarbonate (HCO_3^-) and carbonate (CO_3^-) ions in the tap water which cause an increase in the solubility of CO_2 and acidity of water (Ersoy et al., 2013). Also, according to this study, more portlandite [$Ca(OH)_2$] content may be observed in hydrated pastes having tap water than those mixed with pure water. However, to simulate casting of practical concrete mixtures used in construction and in accordance with ASTM and Canadian Standards, tap water was chosen as the type of mixing water in this study. Authors also suggest that future research could focus on studying the effect of tap water vs. pure (distilled) water on carbonation and resulting hydration products."** With regards to carbon dioxide in the air, the specimen was kept in a clean room inside a pin stub storage box during a 7-day curing period to remove any chance of contamination and exposure to carbon dioxide in the air; and to eliminate the risk of carbonation in the ambient conditions. In addition, authors expect that thinning process also helps to remove enough thickness from possible carbonated surface layer which carbonation can be neglected in the prepared sample for nano-scale investigation. The following statement was also included in the text to address this comment from the reviewer: **"The specimen was kept in a clean room inside pin stub storage box during 7-day curing period to remove chance of contamination and exposure to carbon dioxide in the air; thus, eliminate the risk of carbonation in the ambient conditions.**"
2	Without knowing the chemical composition of the CRM system, the detailed discussions on the chemical compositions would not bring any value to the reader. It is discussed that the focus of the article is on presenting the details and consideration when utilizing sub-micron imaging methods to study the nature of cement-based systems. So, it is suggested to maintain this focus throughout the manuscript and avoid	This comment has been addressed. As mentioned in the text, the chemical compositions of this product are proprietary and not available, however authors added some details in the text to provide a wider insight about this product. **"This is referred to as a modified synthetic CRM which contains Portland cement, reactive silica, calcium and aluminum salts of organic acids and bases, and some crystalline catalysts (Kumar et al., 2009)."**

	getting into the details of the chemical analysis unless authors can share the chemical composition of the base materials.	Also, authors referenced two published articles in the text that describe the chemical compositions and IR spectra of similar product. **"The chemical compositions and IR spectra of similar product have been reported in (Kumar et al., 2009; Sisomphon et al., 2012)."** To keep the focus of the paper on the characterisation techniques using sub-micron images, authors added at various places within the text what would be useful for the readers to know. These details include details of EDS analysis, but the focus has only been on conceivable techniques to visualize the x-ray analysis data and how to obtain information about hydration products and not to draw any conclusions about the CRM materials. Also, in the paper the usefulness of the x-ray analysis to find proper specimens prior to micro fabrication using FIB and later for STEHM study is included. Here are examples of what have been added in the revised text. **"As one of the preparation steps, the x-ray analysis has only been done to select proper location for thinning procedure as well as STEHM investigation and not to draw any conclusions about CRM chemical compositions."** **"Although more sampling from the CRM and its chemical compositions are needed for comprehensive conclusions, the plot of Si/Ca vs Al/Ca in Figure 6-(a) shows that calcium hydroxide ($Ca(OH)_2$) was the main product of selected regions in 7-days hydrated CRM."** **"However, the goal of this work was to establish an experimental methodology as opposed to determining the absolute proportions of various elements."** **"Moreover, EDS analyses for un- and hydrated CRM for 7-days are plotted as atomic percentage, another way of data representation, normalized to 100%, in Ca-Si-(Al+Mg) ternary diagram in Figure 7."** **"Generally, preliminary experiments have shown that determination of specimen's composition by EDS combined with STEHM is feasible, however, the variability of Ca and Si was too severe to allow fully quantitative results to be presented from these initial experiments."**
3	Since the goal of the manuscript is to establish experimental methodology, it is essential to have several samples prepared	Authors would like to thank the reviewer for such valuable point and agree with the reviewer's point about need of more samples to draw more precise conclusions;

	for each experiment to address the 'consistency' and 'repeatability' issues inherent to analytical methods. This is even more critical for the case of cement-based materials known to have a very low degree of homogeneity (due to the presence of independent and separate phases in the hydration products) and can cause variable observations when looking at different spots within the same specimen. It is also suggested to prepare samples with varied parameters (e.g. thickness) and study their characteristics using different variables adjusted in the utilized techniques such beam energy level and magnification to draw more precise conclusions on the applicability of these experimental methods in the study of cement-based materials.	however, the specimen was divided into five different regions to increase the reliability of the proposed method. Also, the STEHM microscope used in this study is one of the most stable and high-resolution microscopes in the world which provides reliable results and best quality images, but the cost and resources associated with microscope are quite high and as such preparation of more samples needs more funding resources which was not available to the authors. Authors believe the proposed experimental methodology itself, is a quite novel and well-documented technique that will add enough value to current state of knowledge in the study of cement-based materials. Authors are in agreement with the reviewer and hence the following sentences were also added to the text: **"It should be noted that even though one sample was mounted on the stub, the sample was divided into five areas, thus increasing the reliability of the results."** **"Overall, the safe statement that can be made at this point is that SAED patterns of observed CRM particle show amorphous structure; however, more samples are required to be prepared for a comprehensive conclusion."**

Highlights

- Developmental changes in the morphology and internal structures of a concrete repair material used for waterproofing cementitious materials were observed.
- Step-by-step practical procedures for fabrication, analytical examination, wide-field microscopic imaging and nano-scale engineering of cementitious repair materials are provided.
- Hydration products, chemical elements and electron diffraction patterns of waterproofing cementitious repair material were evaluated.
- Scanning Electron Microscopy (SEM), Focused Ion Beam (FIM) system, and Scanning Transmission Electron Holography Microscopy (STEHM) were used as tools for qualitative and quantitative analysis of the repair material.

Specimen Preparation for Nano-scale Investigation of Cementitious Repair Material

Pejman Azarsa [a], Rishi Gupta [a,*]

[*] Corresponding author. Tel.: +1 (250) 721 7033
Email address: guptar@uvic.ca (R. Gupta)

[a] Civil Engineering department, University of Victoria, Victoria, BC, Canada

Abstract

Cementitious Repair Materials (CRMs) in the construction industry have been used for many decades now and has become a very important part of activities in cement world. The performance of some of these CRMs when applied to retrofitting concrete structural elements is also well documented. However, the characterization of some of the CRMs at the micro- and nano level is not fully documented. The first step to studying materials at the microscopic level is to be able to fabricate proper specimens for microscopy. In this study, a special and newly developed class of CRM was selected and fabricated by Focused Ion Beam (FIB) using well-known "Lift-out" technique. The prepared specimen was later examined using various analytical techniques such as energy dispersive x-ray analysis using one of the highest and most stable Scanning Transmission Electron Holography Microscopy (STEHM) around the world. This process enabled understanding of the composition, morphology, and spatial distribution of various phases of the CRM. It was observed that the microstructure consisted of a very fine, compact, and homogenous amorphous structure. X-ray analysis indicated that there was considerable deviation between the Si/Ca ratios for the hydrated product.

Keywords

Specimen Preparation, Focused Ion Beam, Cementitious Materials, Scanning Transmission Electron Holography Microscopy (STEHM), Electron Diffraction Pattern

1 Introduction

Understanding the material structure of new materials at sub-micro scale, can lead to improved development of such materials for the construction and building industries. In order to examine properties of these materials at micro (or Nano) scale, it is essential to observe their morphology, particle size, chemical compositions, and physical characteristics (Sharif, 2016). Nowadays, nano characterization of novel construction materials has become a significant field of research (Sharif, 2016). In particular, the nanoscopy techniques utilizing electron microscopes are the most commonly used methods for cement-based materials.

The electron microscope is a microscope that uses a beam of high voltage electron to create an image of the sample. Electron microscopes are typically used to examine the micro-structure of a wide range of biological, inorganic, metallic, crystals, polymers, or cementitious materials. By utilizing electromagnetic and/or electrostatic lenses to control path of the electrons, they enable the observation of much smaller objects in finer details. For research related to cement-based building materials, currently, SEM has been heavily used instrument for better understanding of the materials' composition, morphology, topography, and also for obtaining crystallographic information. Despite the fact that combination of higher magnification, larger depth of field, and greater resolution makes SEM one of the most powerful tools in research areas and industries dealing with construction materials (Sharif, 2016), yet there are certain limitations in using SEM for investigating materials' properties especially at the atomic level when compared to TEM, which allows an evaluation of the internal structure and spatial distribution of the various phases. In high resolution, the TEM imaging capability allows the instrument's operator to observe fine details (Sharif, 2016). The current TEM systems can inspect in atomic level, which is in the range of 1nm or less as compared to the resolution of SEM which is about tens of nm for common materials. Also, TEM can identify many characteristics of the sample, such as morphology, crystallization, stress, or even magnetic domains (holography) but common SEM only scan a specimen surface which mainly provides information about its morphology.

In contrast to TEM, the specimen preparation of SEM is much simpler. Many materials can be directly loaded in SEM for inspection and some insulating materials require an additional coating. On the other hand, TEM sample preparation is a challenging task as specimens need to be thinned to thickness of 100 nm or less. However, the complex multiphase nature of hydration products in cementitious materials makes

the preparation of specimens thin enough, for electron penetration and TEM examination, far from trivial (Richardson and Groves, 1993). The thinning procedure is very time consuming and it can be done by mechanical breakup and dispersion of the solid (Grudemo, 1964; Lachowski and Diamond, 1983; Lachowski et al., 1980, 1981), replication of fracture surface (Ciach et al., 1971), mechanical thinning (Jennings and Pratt, 1980; Taylor et al., 1985) or abrasive and ion-beam milling (Card et al., 1980; Dalgleish and Ibe, 1981; Dalgleish et al., 1980; Groves and Rodger, 1989; Groves et al., 1986; Jennings et al., 1981; Tiegs, 1975). In the past few years, there has been an upward trend in the use of the Focused Ion Beam (FIB) system which is also adopted in the present work to fabricate a specimen with consistent thickness for TEM examination. By utilizing ion-beam thinning, among other techniques, Jennings et al (Jennings et al., 1981) could obtain information on the morphology of hydrated Tri-calcium Silicate (C_3S) pastes. Dalgleish and Ibe (Dalgleish and Ibe, 1981) also performed some qualitative analyses of Portland cement pastes thinned by ion-beam milling tool. Groves and co-workers (Groves and Rodger, 1989; Groves et al., 1986) have obtained the thinning procedure of hardened cement pastes using ion-beam milling. Through ion-beam thinning process, the possibility of developing artificial defects during the specimen preparation stage must be wisely considered. The drying impact of the vacuum of the ion-beam thinning apparatus and carbon evaporation chamber is inevitable, as the microscope also operates at high vacuum, it must be realized that any observed morphologies relate to a dry state (Richardson and Groves, 1993).

In previous studies, TEM has been used to observe structures of Di-calcium Silicate (C_2S) and Tri-calcium Silicate (C_3S) at sub-micro scale and examine cement hydration products in the form of dispersed particles or crushed specimens (Card et al., 1980; Grudemo, 1964; Grutzeck and Roy, 1969; Lachowski et al., 1980, 1981). TEM has also been operated to identify both inner and outer product regions of the C-S-H phase. The hydration of dispersed cement fragments has been imaged in an environmental cell by high-voltage TEM (Double et al., 1978), but all these previous studies have not considered the fact that the cement particle is typically too thick to enable its internal structures to be fully observed under TEM. As mentioned by Jennings et al. (Jennings et al., 1981), the abovementioned techniques have limitations in terms of loss of spatial relationships and limitation to a fracture path, respectively. This drawback was overcome with ion-beam milling by Javelas et al. (Javelas et al., 1974) on mature mortars and later by Dalgeish et al. (Dalgleish and Ibe, 1981) on mature cement pastes. Furthermore, TEM has been extensively used by Groves (Groves, 1986; Groves et al., 1986), Henderson (Henderson and Bailey, 1988), Rodger (Rodger and Groves, 1989) and Richardson (Richardson, 1999, 2002, 2004, Richardson and Groves, 1992, 1993). These studies have generally focused on both fresh and mature cementitious materials, hydrated for 2 hours or more. Many of the main features and hydration products in a mature ordinary Portland cement (OPC) paste were identified by Rodger and Groves using TEM with microanalysis (Rodger and Groves, 1989). Over a range of Ground Granulated Blast-furnace Slag (GGBS) incorporated with OPCGGBS/OPC, a linear relationship has been observed between an increase in the R/Ca ratio (where R is a trivalent cation, mainly Al_3) and an increase in the Si/Ca ratio (Richardson and Groves, 1992, 1993). Through TEM, early age hydration product shells around cement grains were also studied by Gallucci et al. (Gallucci et al., 2010). In their results, the Ca/Si ratio of C-S-H gel was determined to be 2.8-3.5, which is contrary to findings of other previous studies. Plank et al. (Plank et al., 2006) investigated the intercalation product, composed of AFt and AFm with organic polycarboxylate (PC) polymers using TEM. Its raw material was pure mineral and the intercalation product was synthesized in specified condition.

The size distributions, as a factor to be considered for nanomaterials, can be envisaged with TEM (Borchert et al., 2005; Lin et al., 2008; Sun et al., 2005; Zhang et al., 2004; Ziel et al., 2008). Hou et al. (Hou et al., 2015) studied the effects of colloidal nano-SiO_2 (CNS) with a mean particle size of 20 nm and its precursor, tetraethoxysilane (TEOS), on the transport properties of hardened cement pastes with various *w/c* ratios. TEM morphology micrograph in this study indicated that CNS particles are generally round in shape and well-dispersed, however, agglomeration are also observed. Monitoring the interaction between various components of a mixture can be also clearly achieved by TEM. For instance, the microstructure of fly ash binders incorporated by cement kiln dust (CKD), a by-product of the cement industry, was investigated

under a TEM (Chaunsali and Peethamparan, 2013). Through TEM work, the morphology of calcium alumino-silicate hydrate (C-A-S-H) gel present in the CKD-based fly ash binders, was evidently observed to be fibrillar type. To identify crystalline phases for cement paste at an age of 90 days, Ramezanianpour et al. (Ramezanianpour et al., 2014) used TEM in bright field mode. In their TEM micrographs, hexagonal portlandite ($Ca(OH)_2$) crystalline cubes and aragonite ($CaCO_3$) was observed. Recently, there is an upward trend among physical and biological science disciplines to use TEM for real-time observations of materials interactions in their native fluid environment (Xin et al., 2013). For the in-situ transformation observation, Xin et al. (Xin et al., 2013) embedded their sample inside a micro-fabricated cell with electron transparent membranes in order to contain the fluid in the high vacuum environment of the microscope.

With the development of SEM and TEM, the associate technique of Scanning Transmission Electron Microscopy (STEM) was first described in 1938 by Manfred von Ardenne and later re-investigated at University of Chicago by Crewe et al. (Crewe et al., 1969) with advancement of the field emission gun and adding a high-quality objective lens. Using annular dark-field imaging, Crewe was able to image single heavy atoms on thin carbon substrates (Crewe et al., 1970). Later, the first attempt on cementitious materials at early age was made using STEM to observe the formation of separated shells around reacting cement grains in samples as young as 5h (Scrivener, 1984; Scrivener and Pratt, 1983). Mixtures of mono-phased grains of C_3S, C_3A and hemi-hydrate were also studied using STEM in Scrivener and Pratt's work (Scrivener and Pratt, 1984). At 1-day of hydration, they noticed gaps of up to 10 μm between C_3A grains and their hydration shells while there was a close contact between the C_3S grains and hydration products. This difference in behavior between cement and mixtures of pure phases indicates that the hydration process is influenced by the anhydrous phases within the cement grains (Scrivener and Pratt, 1984). Although, STEM and SEM have been widely used to examine and review the micro-level structure of cement-based materials for building and construction industries, the manufacturing procedures and quantitative techniques for microscopic level investigation using STEM have not been reported in detail in any present-day literature. Hence, the authors have attempted to investigate the microstructure of CRM that contribute to bond cracks together to identify its morphology, chemical compositions, and obtain crystallographic information of this material.

The objectives of the current study are to provide better understanding about fabrication and examination of a cement-based repair material at sub-micro scale as well as detailed characterization of its morphology, composition and structure using one of the highest resolution STEHM in the world as the main tool of investigation. Through this paper, the fabrication process and STEHM analyses of ion-thinned CRM sample, cured and activated for 7-days by spraying water, are also explained in Section 2, followed by obtained results and discussion presented in Section 3. This study is expected to be of significant value in the investigation of the CRMs' nanostructure and the composition of hydration product, and thus may provide a valuable tool in understanding and further development of these construction materials.

2 Experimental Program

2.1 Materials

A Cementitious Repair Material (CRM) has been selected in this study for STEHM examination. This is referred to as a modified synthetic CRM which contains Portland cement, reactive silica, calcium and aluminum salts of organic acids and bases, and some crystalline catalysts (Kumar et al., 2009); a special category of repair material commercially produced and used for waterproofing cementitious materials. However, the chemistry of this product is proprietary and available. The chemical compositions and IR spectra of similar product have been reported in (Kumar et al., 2009; Sisomphon et al., 2012). Some of the physical properties of the material, reported by its manufacturer and used in this study, are given in Table 1. It should be noted that the focus of this paper is to further develop the specimen fabrication technique and not so much to characterize one particular type of CRM.

Table 1: Physical properties of CRM

Color	Gray
Texture	Powder
Particle size	40-150 μm
Bulk density	1.2~1.5 g/cm^3
pH	13 (when mixed with water)
Solids	100%

2.2 Specimen preparation

Any specimen for STEHM analysis must be of an appropriate size with thickness less than 50-100 nm in order to allow passage of electrons for imaging sample's internal structure. As noted in Table 1, the average particle size of anhydrous CRM powder is reported by its supplier to be about 40-150 μm. Hence, the main obstacle was to prepare an appropriate size specimen that can easily fit inside the STEHM chamber. This requires CRM particles to be cut and thinned. Prior to the thinning procedure, anhydrous particles were dispersed and mounted on aluminum stub covered with carbon paste (Figure 1). Although the anhydrous particles' size reported by its supplier is about 40-150 μm, it should be noted that the particles' size measured from SEM images turned out to be above 20 μm and less than 1.5 mm. Hence, picking a suitable particle size for thinning procedure was quite a challenging task. The SEM and X-ray analyses of dispersed particles were later performed on raw material using Hitachi S-4800 SEM equipped with Burker Quantax EDS system for X-ray spectroscopy.

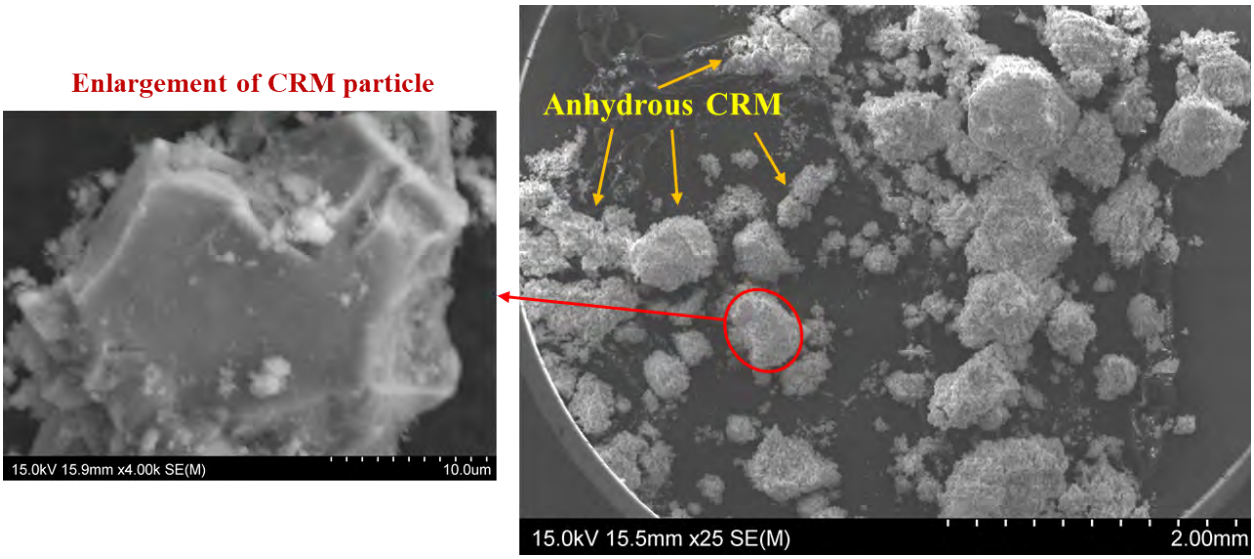

Figure 1: *SEM micrograph of anhydrous CRM particles (Magnification: x25)*

For investigation of hydration products, the specimen was prepared by spraying with tap water for a period of 7 days (three times per day) to activate the hydration of the CRM crystals. It is reported that there can be some negative effects of using tap water instead of distilled water. Negative effects reported include: decrease in initial and final setting time mainly due to flocculation process on setting and reduction in pH level of the paste due to presence of bicarbonate (HCO_3^-) and carbonate (CO_3^-) ions in the tap water which cause an increase in the solubility of CO_2 and acidity of water (Ersoy et al., 2013). Also, according to this study, more portlandite [$Ca(OH)_2$] content may be observed in hydrated pastes having tap water than those mixed with pure water. However, to simulate casting of practical concrete mixtures used in construction and in accordance with ASTM and Canadian Standards, tap water was chosen as the type of mixing water in this study. Authors also suggest that future research could focus on studying the effect of tap water vs. pure (distilled) water on carbonation and resulting hydration products. The specimen was kept in a clean room inside pin stub storage box during 7-day curing period to remove chance of contamination and exposure to carbon dioxide in the air; thus, eliminate the risk of carbonation in the ambient conditions. The hydrated particles were again imaged by SEM to identify morphology and various phases after 7-days hydration, shown in Figure 2. The enlargement of particles and formation of needle-shape crystals were observed through SEM investigation.

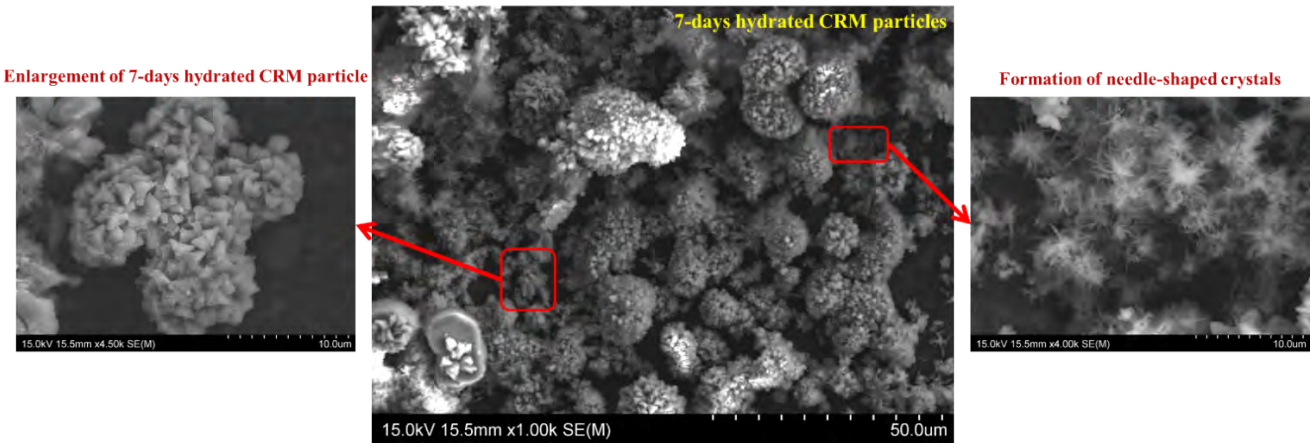

Figure 2: *SEM micrograph of 7-days hydrated CRM (Magnification on the image in the center: x1.00k)*

Thinning processes were conducted by Hitachi FB-2100 FIB system for making micrometer- and nanometer-sized cut in the CRM powder. A well-known sample preparation technique called "lift-out" technique was used to fabricate proper sample size for STEHM imaging. The only requirement for the lift-out technique is that the bulk sample must fit inside the FIB specimen chamber, this condition could easily be satisfied with obtained hydration products. After platinum deposition on sample surface was completed (Figure 3-(a)), a large stair-step FIB trench was cut on one side of the Region of Interest (ROI) and a rectangular FIB trench was cut on the other side of ROI (Figure 3-(b) & -(c)), following similar procedures as reported in (Giannuzzi and Stevie, 1999; Giannuzzi et al., 2005). Before final thinning, the specimen was tilted to >45° and then the bottom, left side, and a portion of the right side of the specimen was cut free. A solid glass rod pulled to a sharp tip (~20–30 µm) was inserted into the arm of a hydraulic micromanipulator. Using the micromanipulator, the membrane was "lift-out" of the bulk sample and was then positioned onto a coated copper (Cu) FIB lift-out TEM grid which is designed for in-situ lift to attach the TEM lamellae milled out by FIB systems. Electrostatic forces allow the membrane to be lifted out by means of the glass rod. TEM grids, with typical thickness of 35 µm/-5 µm, fit all standards TEM holders and provide a full view of the thin section attached to the posts. A grid with three narrow flat posts has been used with identification letters (A-C) were etched into it as schematically shown in Figure 3-(e) & (f). Later, sample was tilted back to its starting position and thinned to electron transparency. A final FIB cut

was performed ~1-2° with respect to the plane of the specimen surface. In this manner, the thinnest portion of the specimen lies in the ROI. The remaining right side of the specimen was milled free leaving the electron transparent membrane lying in the cut trenches. After completing the above-mentioned steps, the specimen was ready for STEHM analysis. It should be mentioned that two individual particles were initially attempted to be mounted on the grid; however, the second attempt for picking and welding the particle to the grid failed. So, only one particle could successfully be welded to the Cu grid. This indicates some of the challenges still encountered during this process.

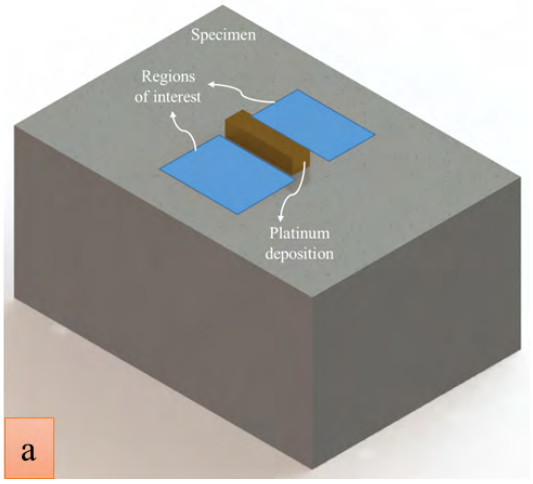

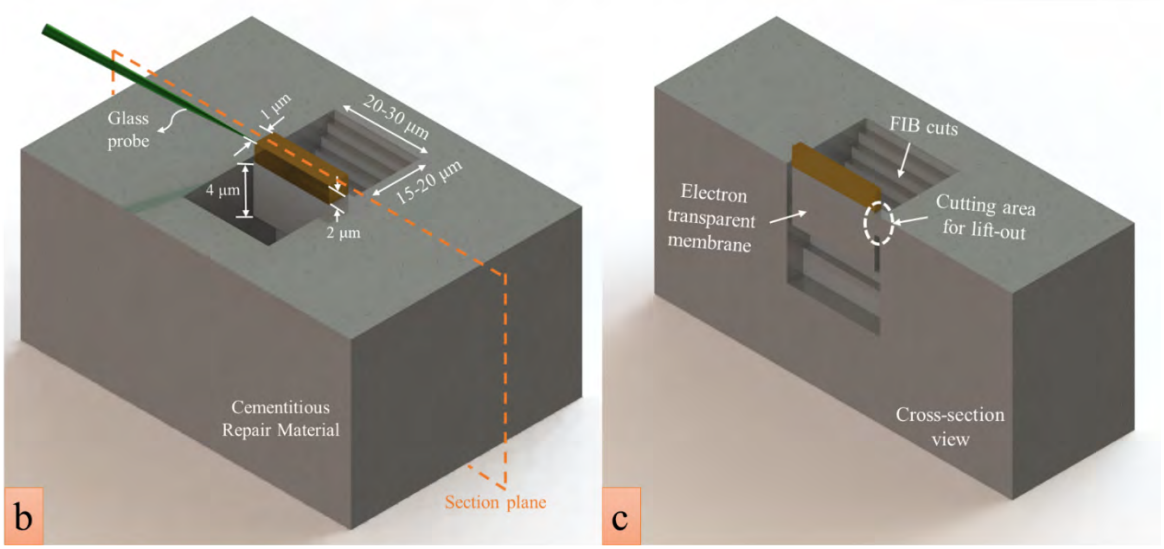

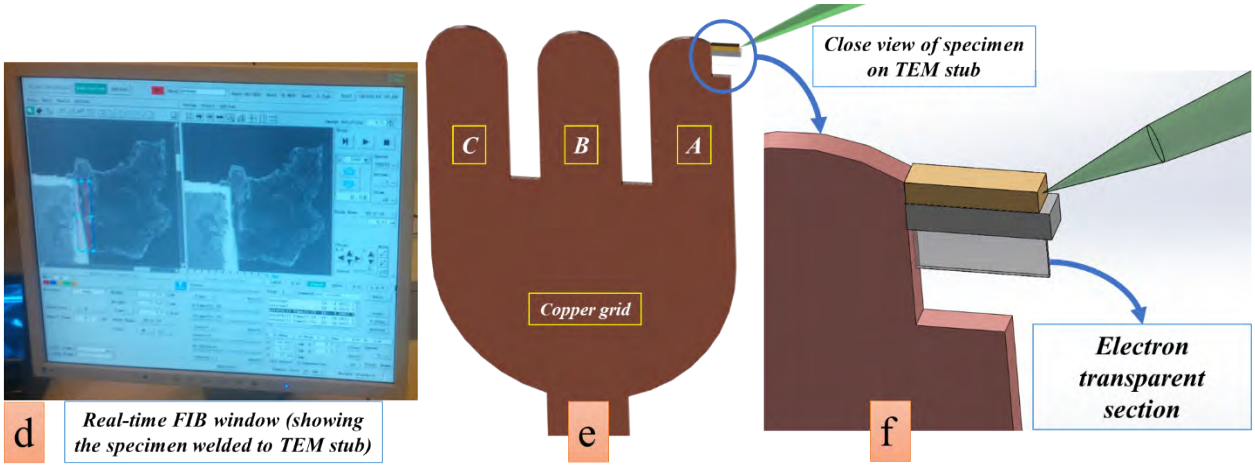

Figure 3: *Schematic and real view of "lifted-out" technique used to manufacture CRM sample*

2.3 Scanning Transmission Electron Holography Microscopy (STEHM)

Structure of the CRM was examined by imaging and diffraction techniques using Hitachi HF-3300v STEHM having spherical + Coma correction of its TEM mode. The STEHM, used through this work, has proven to be the most stable microscope in the world as well as one of the highest resolution microscopes. The operating voltage was 200 kV and the current at the sample surface was estimated to be about 1 nA. STEHM makes it easier to obtain high magnification images without beam damage. Some images were acquired in the dark-field mode, with a high angle annular detector fitted in the microscope; this improves contrast for low atomic weight materials such as cement-based materials. For elemental analysis, STEHM is also equipped with Bruker EDS analyzer at a high take off angle for efficient collection of the X-rays. This enabled analysis to be made without tilting the specimen.

3 Results and Discussion

3.1 EDS analysis using SEM

Prior to FIB fabrication process and imaging with STEHM, the CRM (before and after 7-days hydration) were analyzed using SEM/EDS to identify its morphology, elements inside and hydration products. The x-rays generated can be collected using Energy Dispersive X-ray Spectroscopy (EDS) detector and used to form high spatial resolution elemental maps. Through this study, EDS analysis spots were chosen carefully depending on the morphology of the un- and hydrated phases probed, so that results could be attributed as accurately as possible to pure phases. In this paper, the distribution of different elements of CRM using both SEM and STEHM were identified.

EDS analysis of CRM in selected regions indicated mostly typical elements of cement (calcium, oxygen, and silicon in major amounts, in addition to iron, aluminum, magnesium). SEM photograph and EDS elemental mapping were acquired for anhydrous CRM, shown in Figure 4. The figure provides direct visualization (Figure 4-(a)), elemental mapping (Figure 4-(c) & -(d)) and quantification of elements in raw specimen (Figure 4-(b)). Multi-elemental mapping performed by raster scanning of area marked in SEM image, and taking a spectrum at each point to build up an areal distribution of the elements, indicates very high concentration of Calcium (Ca), Silicon (Si) and relatively high Magnesium (Mg) content, revealing that there is a considerable amount of Mg present in the examined sample. This observation was also confirmed from spectrum in Figure 4-(b) which provides information about what elements are present and the quantities of each. The obtained information from EDS was later used to identify hydration products and attain atomic ratio of the elements. Similar micrograph was obtained for the CRM, hydrated for 7-days (Figure 5).

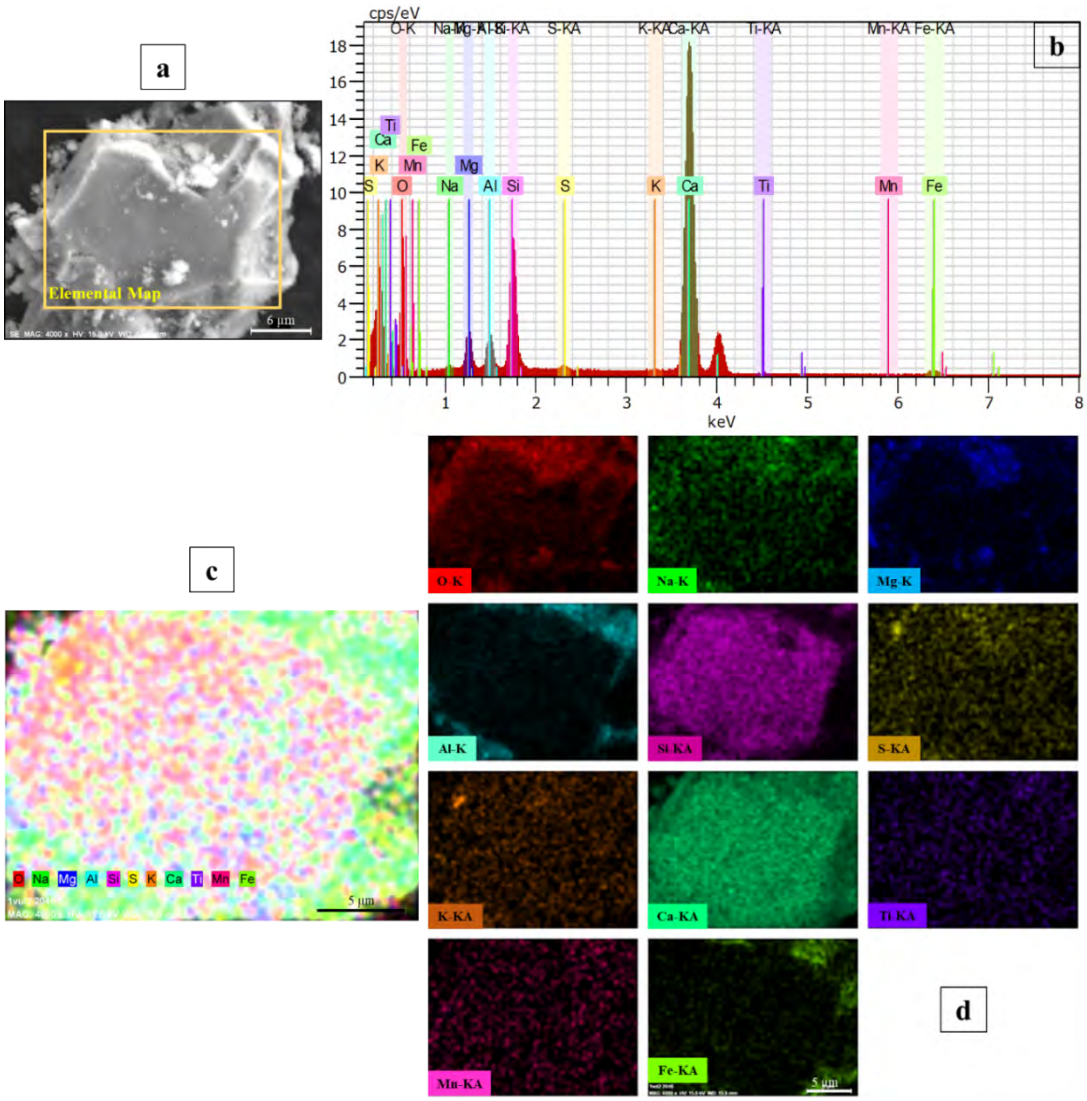

Figure 4: *EDS spectrum, multiple and individual elemental mapping of anhydrous CRM*

After spraying water for 7 days, it was observed with naked-eye that particles swelled on the stub and expanded in size due to the reaction process. Three selected locations in SEM image (Figure 5), where needle-shape crystals were formed, indicate that high amount of Ca exists predominantly compare to other elements. Elemental mapping also reaffirmed these crystals were consisted of mostly Ca. The EDS analysis of hydration product did not show any significant elemental differences with that of un-hydrated one in Figure 4 except only high content of Ca and less amount of Si or Mg; this suggests that in spite of the different morphology of hydrated CRM (e.g. formation of needle-shape crystals, shown in Figure 5), the reaction products are the results of growth in particle size. As one of the preparation steps, the x-ray analysis has only been done to select proper location for thinning procedure as well as STEHM investigation and not to draw any conclusions about CRM chemical compositions. Authors also believe that spraying water for 7-days period might not be enough time and good curing method to get fully hydration product. Hence, authors recommend that CRM needs to be cautiously hydrated by suitable wet-curing method before its intended application since curing is a critical step and plays an important role in obtaining fully performance of cement-based materials. Further investigation on this material is required to understand the effect of various curing methods on morphology and hydration products.

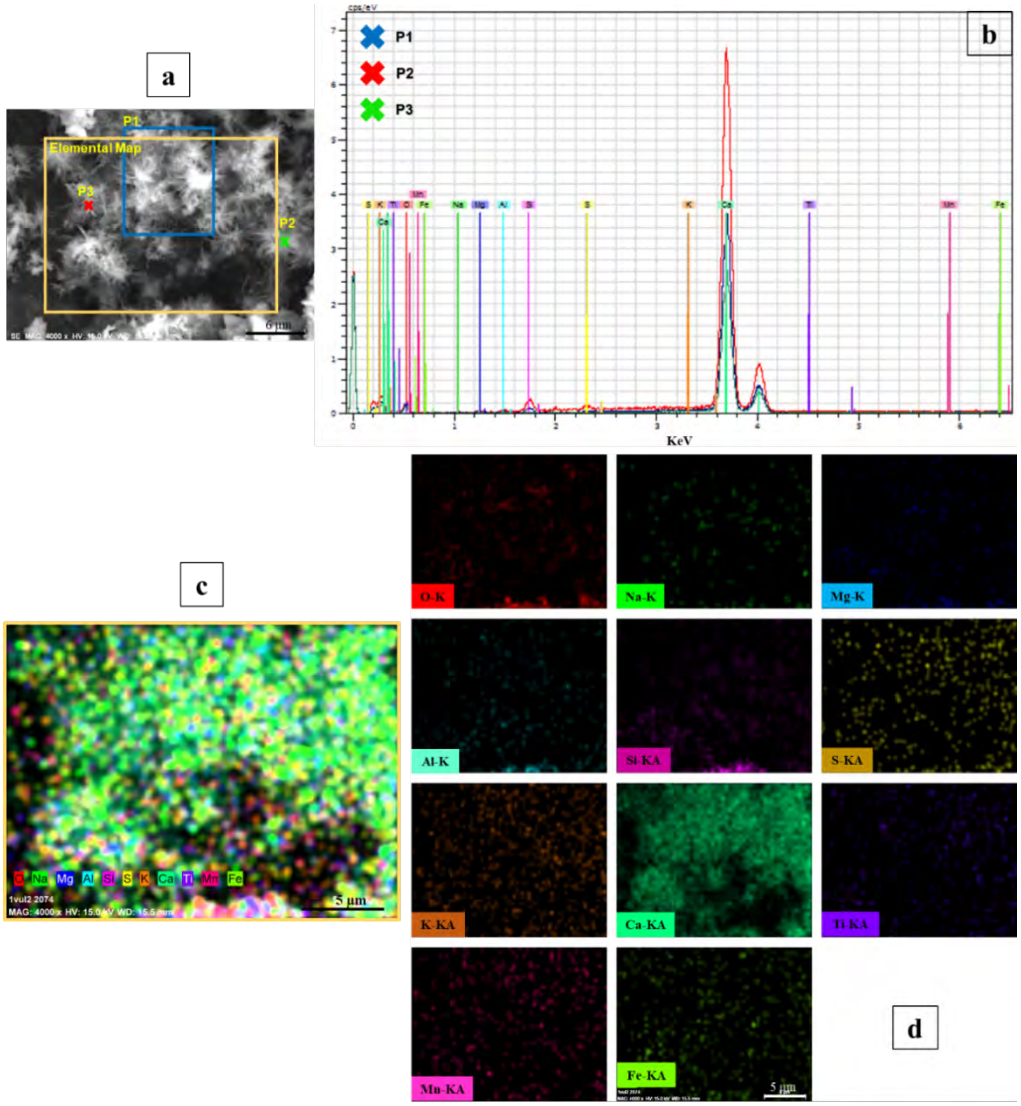

Figure 5: *EDS spectrum, multiple and individual elemental mapping of 7-days hydrated CRM*

One of the ways to present and further analyze the data, and thus hydrated compositions, is graphically, in the form of atomic ratio plot. The plots in Figure 6-(a) & -(b) were obtained from EDS spectra of hydration products by calculating each element's atomic percent from its mass percent for all selected spots, and then presented in the form of a graph after deriving atomic ratios for particular elements. To derive comprehensive analysis, more than 10 different spots were selected and all data points, collected from EDS analysis spectrums, represent a point for Si/Ca vs Al/Ca in one plot Figure 6-(a) and Al/Ca vs S/Ca in Figure 6-(b). It is important to appreciate that the plots quantify the compositions of the hydration product; however, the proportion of each composition present in the paste cannot be quantified.

Although more sampling from the CRM and its chemical compositions are needed for comprehensive conclusions, the plot of Si/Ca vs Al/Ca in Figure 6-(a) shows that calcium hydroxide ($Ca(OH)_2$) was the main product of selected regions in 7-days hydrated CRM. It also indicates that Si/Ca ratio of the sample is approximately between 0.01~0.1 while the Al/Ca ratio is 0.02~0.04. The typical Si/Ca ratio of the inner product C-S-H in neat Portland cement have been widely reported from several characterization techniques, with values ranging from approximately 0.45 to 0.6 while the Al/Ca ratio is 0.04~0.06. Hence, the cluster near origin in Figure 6-(a) & -(b) corresponds to largely CH crystals and rarely C-S-H gel. The plot

demonstrates that no AFt (a group of calcium sulfoaluminate hydrates) and AFm (a group of calcium aluminate hydrates) phases were detected. As the most common and important member of AFt group, Ettringite also forms needle-shape crystals similar to the ones imaged in CRM; however, through authors analyses, the CRM crystals have not been identified to be Ettringite. Figure 6-(b) clarifies the picture considerably. No pure gypsum, a hydrated calcium sulfate in chemical form that helps in compensating the rate of hardening of the cement, is identified.

It is hypothesized that dominant presence of pure CH in hydration products can be rooted in random data collection from various locations. Hence, it is strongly recommended to not collect data from random locations before seeking out visually different hydration phases from SEM micrograph. Furthermore, more spectra for hydrated compositions is required to be collected in order to systematically identify single or more than one phases of hydration product since different forms of these phases can intergrow on a scale smaller than the X-ray excitation volume. However, the goal of this work was to establish an experimental methodology as opposed to determining the absolute proportions of various elements.

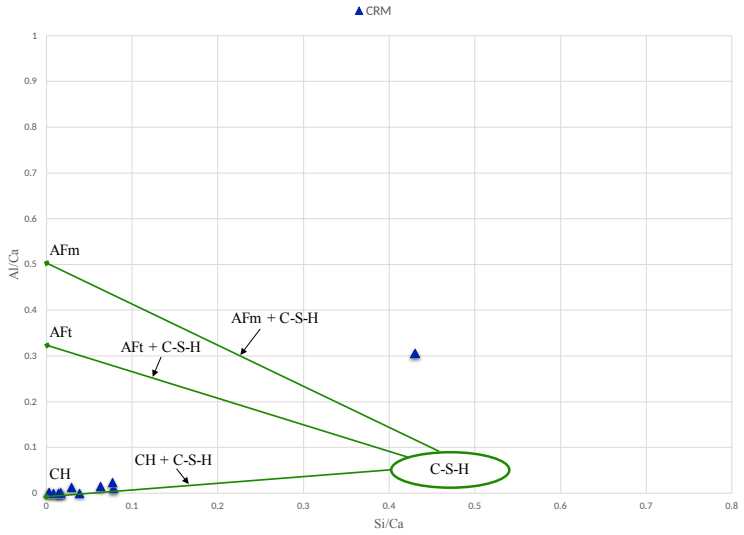

(a)

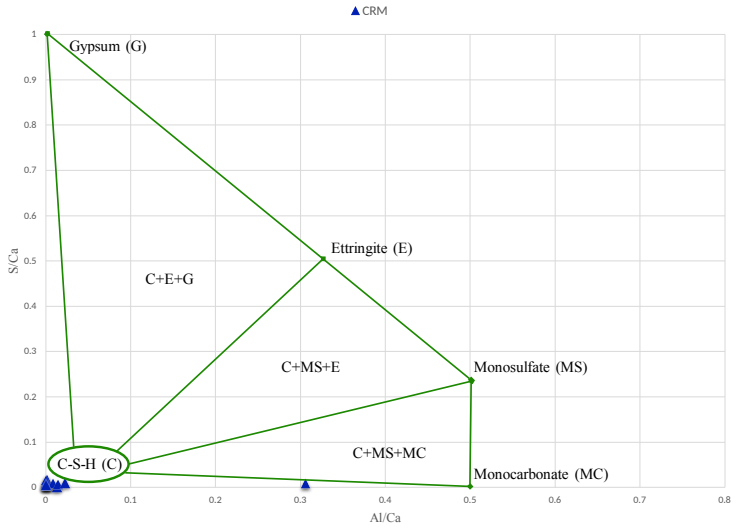

(b)

Figure 6: *7-days hydrated CRM atomic ratio plot of (a) Si/Ca vs Al/Ca (b) Al/Ca vs S/Ca*

Moreover, EDS analyses for un- and hydrated CRM for 7-days are plotted as atomic percentage, another way of data representation, normalized to 100%, in Ca-Si-(Al+Mg) ternary diagram in Figure 7. The analyses of hydration product resulted in identification of dominant phase of CH, similar to data represented in Figure 6. While most data points of hydration products in Figure 7-(b) are located close to the cluster of analyses plotted in Figure 6, the un-hydrated CRM collected spots in Figure 7-(a) are scattered in random directions which makes the conclusion about its phases difficult, and thus requires more data to be collected. For comparison purposes, Portland cement hydration product range is also plotted on the graph.

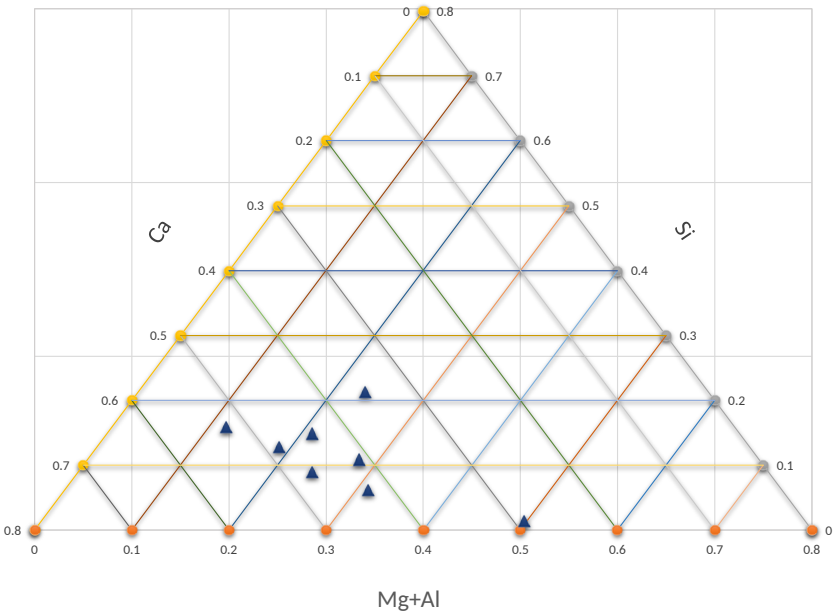

(a)

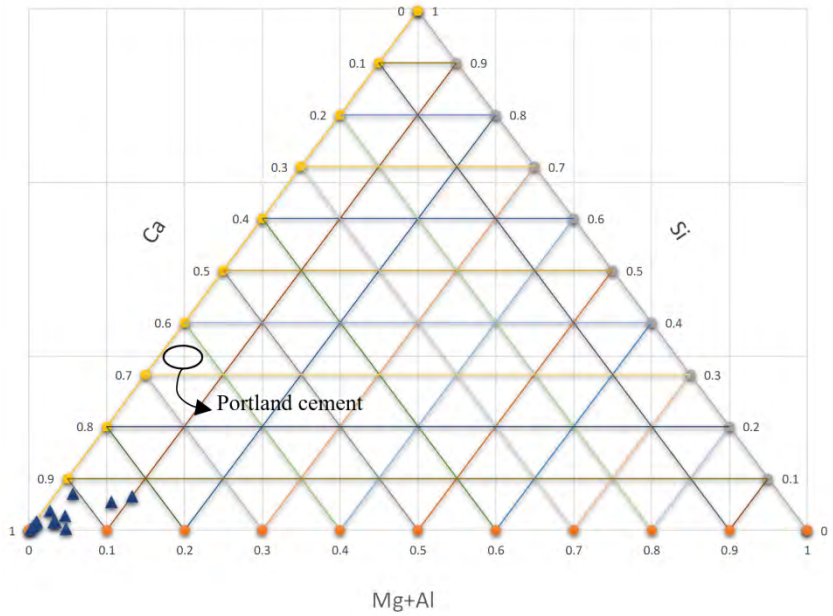

(b)

Figure 7: (a) *Un- and* **(b)** *hydrated CRM Ca-Si-(Mg+Al) ternary diagrams*

3.2 STEHM Micrographs

A CRM with a mean particle size of 80 µm was thinned down into 1~2 µm size using FIB and further magnified in STEHM in order to investigate morphology, element distribution, and structural order of its nano structure. Using STEHM, a highly-focused electron probe was raster-scanned across the prepared specimen to acquire various types of scattering. Figure 8-(a) exhibits a bright-field micrograph, taken in TEM mode from 7-day hydrated CRM specimen, indicating compact, fine-scale, homogenous morphology. Many regions are free of obvious defects and dislocation (dislocation will of course be introduced when the bulk sample is ground to make powder). For further investigation of sample's morphology, it was divided into 5 different color-coded regions (ROI: A-E in Figure 8-(a)) where TEM micrographs were obtained and are explained in section 3.4. In addition, mapping the intensity of high-angle scattered electrons of the CRM using STEHM resulted in formation of Z-contrast micrograph which is incoherent (Figure 8-(b)). Since the image was formed from high-angle scattering of atomic nuclei, the scattering cross section relates to atomic number (Z^2). In Figure 8-(b), areas that appear bright in the specimen correspond to higher atomic weight elements. For example, on the right brighter region of the specimen (illustrated in Figure 8-b by yellow boundary), there are more elements with higher atomic weight like Fe or Al, although, for further element identification, EDS examination was required. Later, EDS analysis on thinned particle using STEHM have been performed to identify elements inside and acquire X-ray spectrum (3.6). Thickness map and crystallographic information were additionally obtained as characterization techniques for further investigation of the CRM structure, and reported in the sections 3.3 and 3.5. It should be noted even though one sample was mounted on the stub, the sample was divided into five areas, thus increasing the reliability of the results.

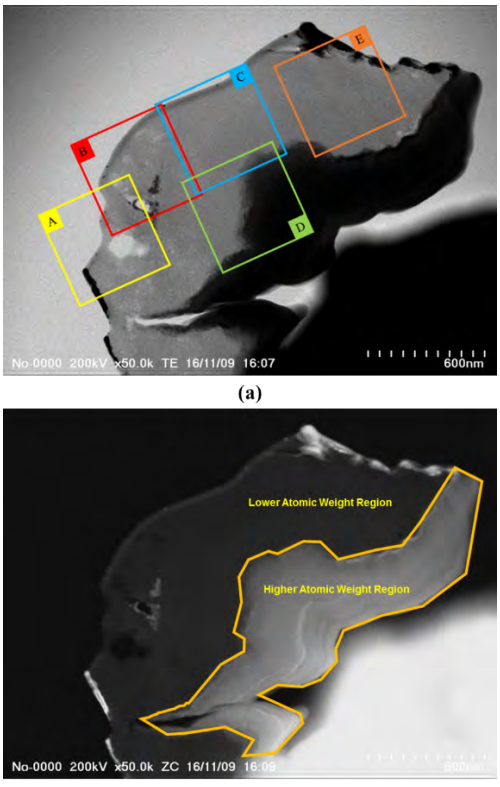

Figure 8: *Seven-days hydrated CRM* ***(a)*** *TEM micrograph (bright-field image)* ***(b)*** *Z-contrast micrograph*

3.3 Relative Thickness Map

It is necessary to check the thickness of fabricated specimen to ensure passage of electrons through the sample. A reliable indicator to overlook is the Mean Free Path (MFP) value, λ, which represents the average

distance a beam electron will travel inside the samples between electron energy loss scattering events for inelastic scattering which contributes to significant details at the atomic level to high resolution images particularly in high voltage instruments. For a specimen of thickness *t*, the average number of times, an electron beam will scatter in-elastically, is t/λ.

To obtain thickness map for the CRM particle, two images, one unfiltered image without introducing an energy-selection slit that is inserted into the energy dispersive plane of an energy filter, which selects electrons having specific energies and another filtered (zero-loss) image by introducing the energy selecting slit around the zero-loss energy (with slit width 10 eV) were acquired. Then, the relative thickness map obtained from these two images using the log-ratio method in Gatan Digital Micrograph provided the local sample thickness in units of inelastic mean free path (λ). The relative thickness map and corresponding average intensity profile were obtained for ROIs (A-E) of the particle at 200 keV incident energy, shown in Figure 9. The MFP values for most of ROIs A-C and E are in the range between 0.4-0.7. Knowing the λ values for 7-days hydrated CRM, the sample thickness, *t*, was measured to be 50-80 nm. The obtained $^{t}/_{\lambda}$ value indicates the suitability for the ROI area for transmitting electrons through specimen and performing Electron Energy Loss Spectroscopy (EELS) studies since its value provides a direct indication of the degree of signal degradation by plural scattering independent of the sample composition. Similar approach can be performed in Energy Filtered TEM (EFTEM) to generate a two-dimensional $^{t}/_{\lambda}$ map.

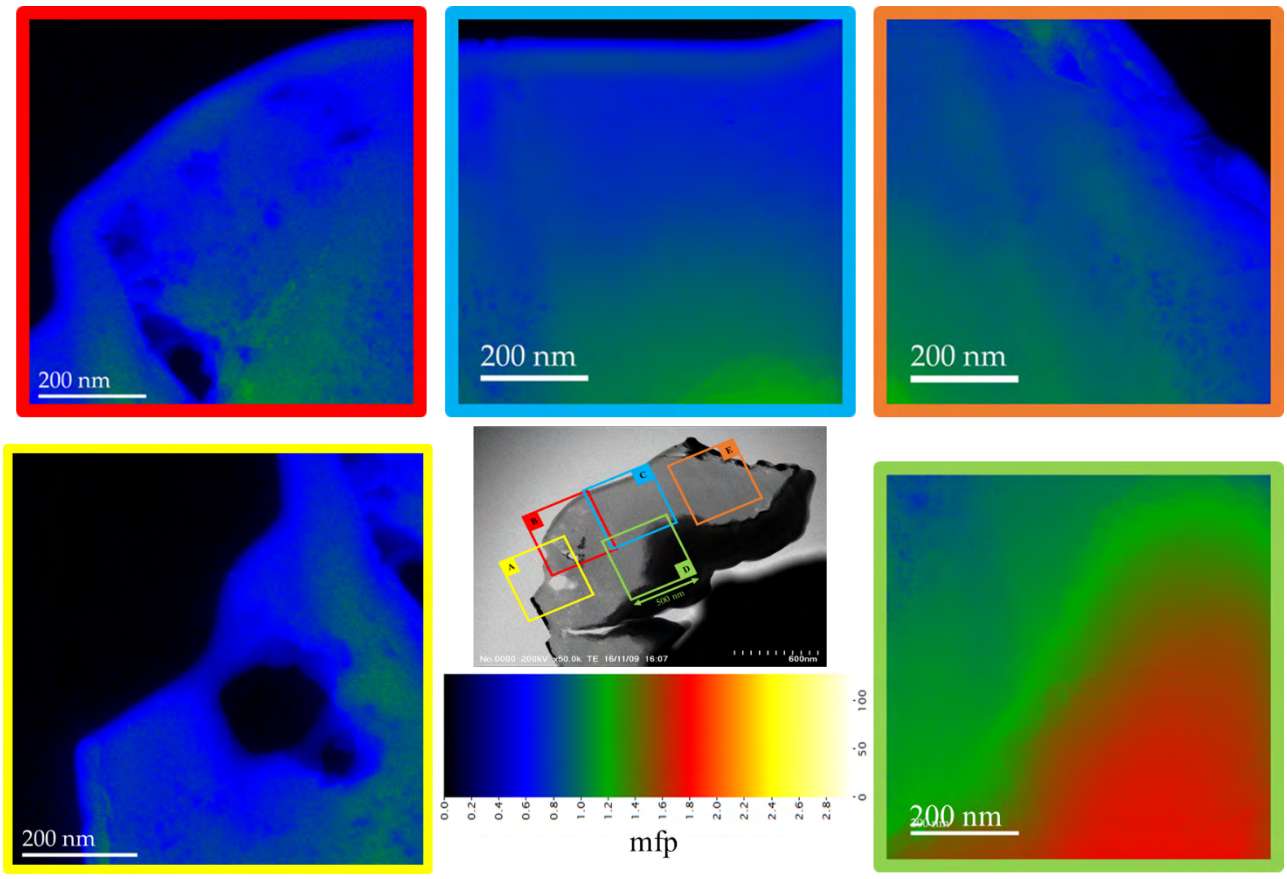

Figure 9: *Relative thickness map of selected CRM particle regions*

3.4 Morphological aspects of hydration products

The morphological characteristics of hydrated CRM were acquired for five color-coded (500×500 nm^2 square) ROIs (Regions: A-E) under STEHM. All ROIs were nearly devoid in the TEM micrograph except

ROI-A that has double holes with 150-200 nm size. No quantitative significance can be attached to the hole sizes seen on the micrograph since the holes' structure were initially observed to exist and coarsen as a result of electron beam damage. The amount of damage suffered in a very short time, due to electron beam, was sharply evident in the ROI-B micrograph, appearing brighter in Figure 10; however, we were still able to get clear satisfactory images. Also, no morphology other than a fine structure is seen within ROI-C of TEM micrograph. It is hypothesized that large quantities of crystals, observed in Figure 2, which were highly hydrated, might have readily decomposed during FIB fabrication and specimen preparation. In the region D, evidence of contamination from electron beam was observed as well. It must be noted that the morphology of prepared specimen just brought into field of view may have sustained preventable damage, not only from sample preparation technique, but how the beam had been manipulated over the sample. For instance, if the beam current is initially turned up at low magnification with a large spot size and poorly defocused electron beam, then an extensive area can be damaged (Richardson and Groves, 1993). Hence, an operator who implements the proposed sample preparation technique and nano-scale investigation, needs to consider sufficient cautious in all steps to avoid any damages to the sample.

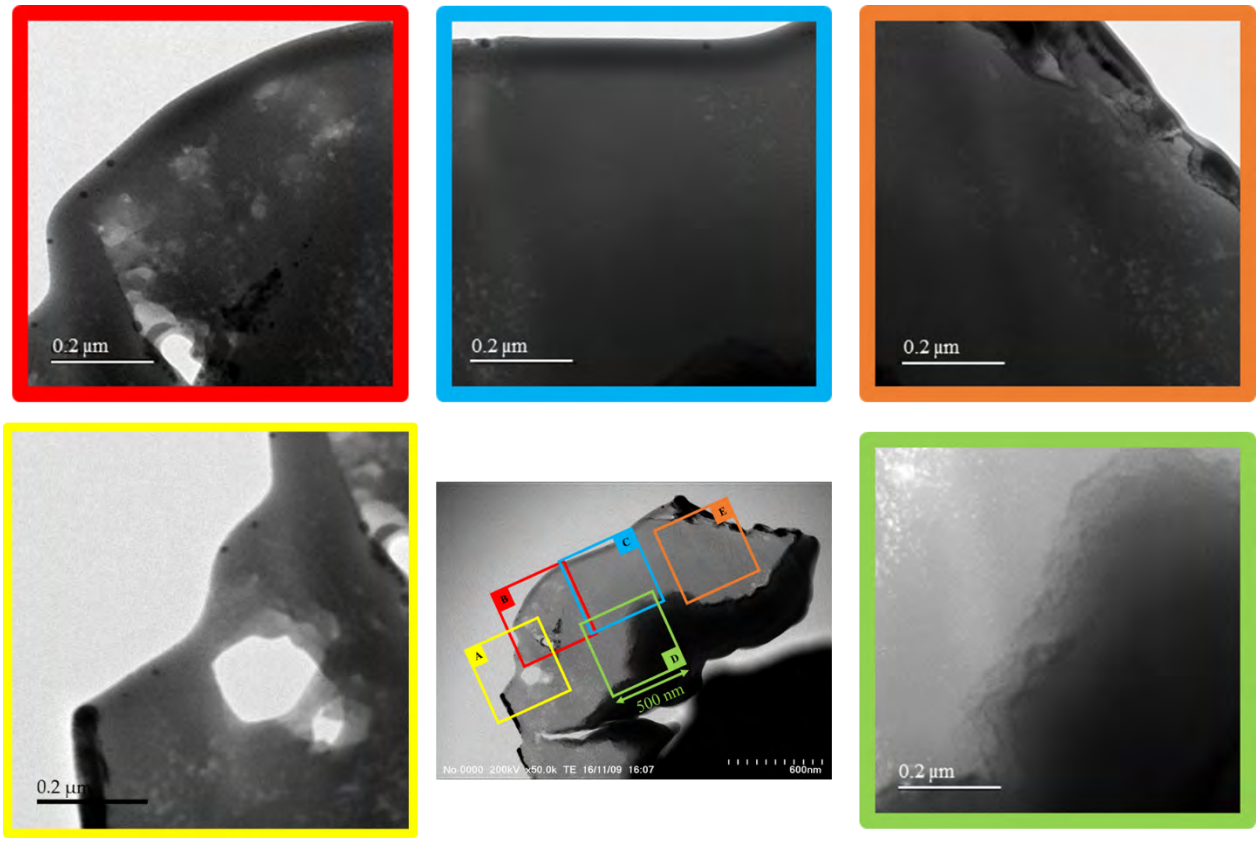

Figure 10: *TEM micrograph of color-coded selected regions of CRM specimen*

3.5 Selected Area Electron Diffraction (SAED) Pattern

Selected Area Electron Diffraction (SAED) patterns can be obtained from localized regions of the sample by inserting a selected area diffraction aperture into the image plane of the objective lenses. SAED patterns help to determine whether a specimen is single crystal, polycrystalline, or amorphous. The sampled 7-days hydrated particle was studied using SAED to ensure the presence or absence of crystalline phases. SAED patterns were obtained from five various selected regions (ROI: I-V) within the boundary and inner-body of the particle, shown in Figure 11. The area covered by a SAED aperture was 100-120 nm in diameter. Inspection of these patterns led to some very interesting findings. In spite of the complex appearance of this microstructure, SAED patterns of all regions show that most of the diffracting material has amorphous

structures. This observation is also confirmed by intensity profile of SAED patterns, as illustrated in Figure 11. As an additional characterization technique, a simple XRD examination can be also performed to identify non-crystalinity of the hydrated CRM particle. Part of difficulty in the reliability of the SAED investigations may relate to amorphization of the specimen by the ion beam milling process and/or beam damage in the microscope (Viehland et al., 1996). Groves et al. (Groves et al., 1986) successfully achieved the thinning of Hardened Cement Paste (HCP) specimens by ion-beam methods, using a liquid-nitrogen-cooled stage-to minimize thermal damage- and a slow thinning rate. They were able to obtain reproducible results in their investigations. They also noted that the possibility of thermal damage during preparation is more serious than beam damage in the microscope, because the damage accumulated in the microscope can be monitored *in situ.*

Diffuse rings, evidence for short-range structural order and sub-crystalline region in specimen were observed in region I, IV and V using SAED (indicated by yellow arrows); however, further investigation of the hydration product, as also performed by Viehland et al. (Viehland et al., 1996) for the C-S-H gel phase, require to be conducted to better understand the midscale structural units that result in short-range ordering, seen in the marked areas with arrows in the SAED patterns. Presence of nanocrystallinity region can be indicated in sample's structure through High Resolution Electron Microscope (HREM) studies and its development inside specimen may occur very rapidly at short times, slowing down, as sample ages. Similar results have been reported for C-S-H gels for freshly cured and aged gels (Viehland et al., 1996). Their results supported the arguments that system becomes metastably trapped in a sequence of near-degenerate states because of the inability to undergo long-term diffusion. Overall, the safe statement that can be made at this point is that SAED patterns of observed CRM particle show amorphous structure; however, more samples are required to be prepared for comprehensive conclusion.

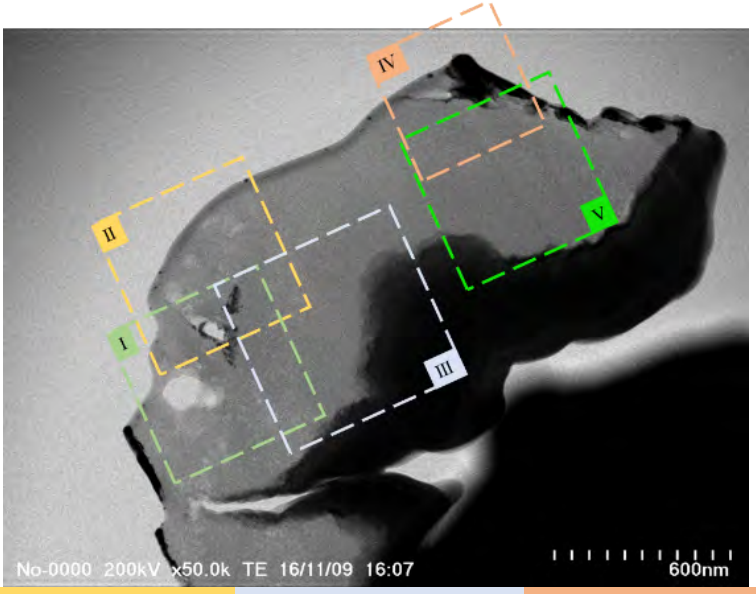

ROI	Region I	Region II	Region III	Region IV	Region V

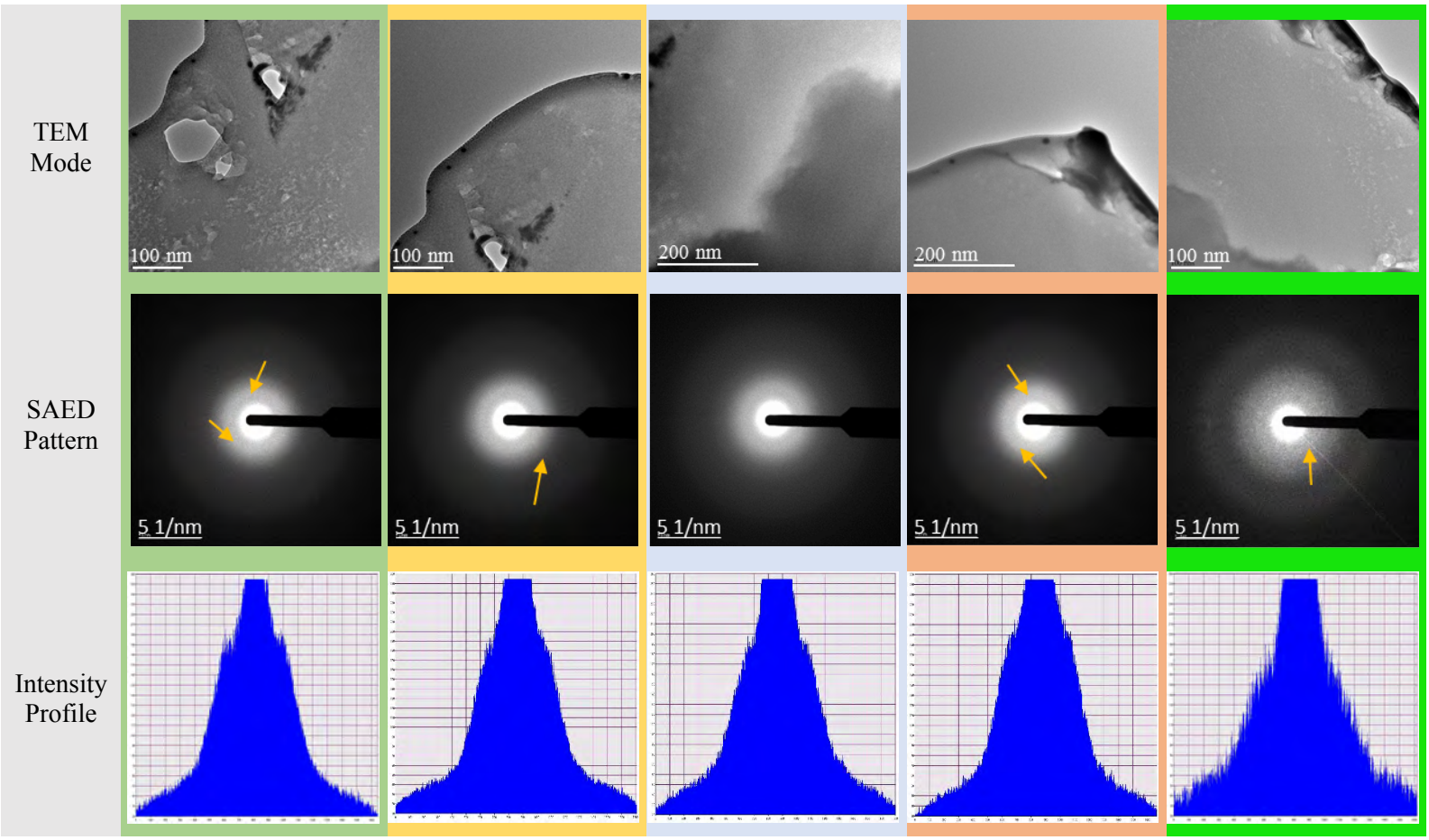

Figure 11: *Selected Area Electron Diffraction (SAED) pattern of CRM particle and its intensity profile*

3.6 EDS analysis using STEHM

EDS analysis was performed by STEHM on fabricated specimen to investigate the elemental distribution, confirm observations from SEM/EDS analysis and calculate Ca/Si ratio of examined particle. The size of the mapping area was chosen to be about 2×2 μm^2 (Figure 12-(a)) and the X-ray mapping involved the simultaneous analysis of eight elements (O, Ca, Si, Mg, Fe, Al, Ga, W) (Figure 12-(c)). EDS elemental maps show that the specified region of the specimen mainly contains silicon and calcium together with small amounts of aluminum and iron, shown in Figure 12-(d). It should be mentioned that calcium was not detected by EDS on the right side of specimen area. Iron (Fe) was also present throughout the selected region, but did not appear to be particularly associated with either aluminum or magnesium. Iron contents occurred in the right area were higher. Additionally, the amount of magnesium, originally presents in the anhydrous sample, was not significant in EDS elemental map. In Figure 12-b, the spectra, acquired from the investigated particle, shows high peak for Si and Ca. Evidence of Gallium (Ga), most likely sputtered from electron beam, was also observed in different spots which cautiously needs to be prevented during sample preparation as it makes EDS analysis of investigated sample less appealing. The Ca/Si ratio of the particle was calculated to be about 0.4–0.6. In reviewing previous TEM work by the authors (unpublished), it was noted that no similar cement hydration products contain substantial silicon content. The low Ca/Si ratio measured was interpreted as being due to one or more of the following: (a) the fine intermixing of Wollastonite ($CaSiO_3$), Quartz (SiO_4), or Silica (SiO_2), (b) residual undissolved silicon calcium particles, or (c) the less coexistence of tobermorite (T2) and jennite (J2) like structures (Gallucci et al., 2010). Also, the Ca/Si ratio has been reported previously to depend on the beam acceleration voltage, indicating the influence of beam-spreading effects (Taylor, 1997). Generally, preliminary experiments have shown that

determination of specimen's composition by EDS combined with STEHM is feasible, however, the variability of Ca and Si was too severe to allow fully quantitative results to be presented from these initial experiments.

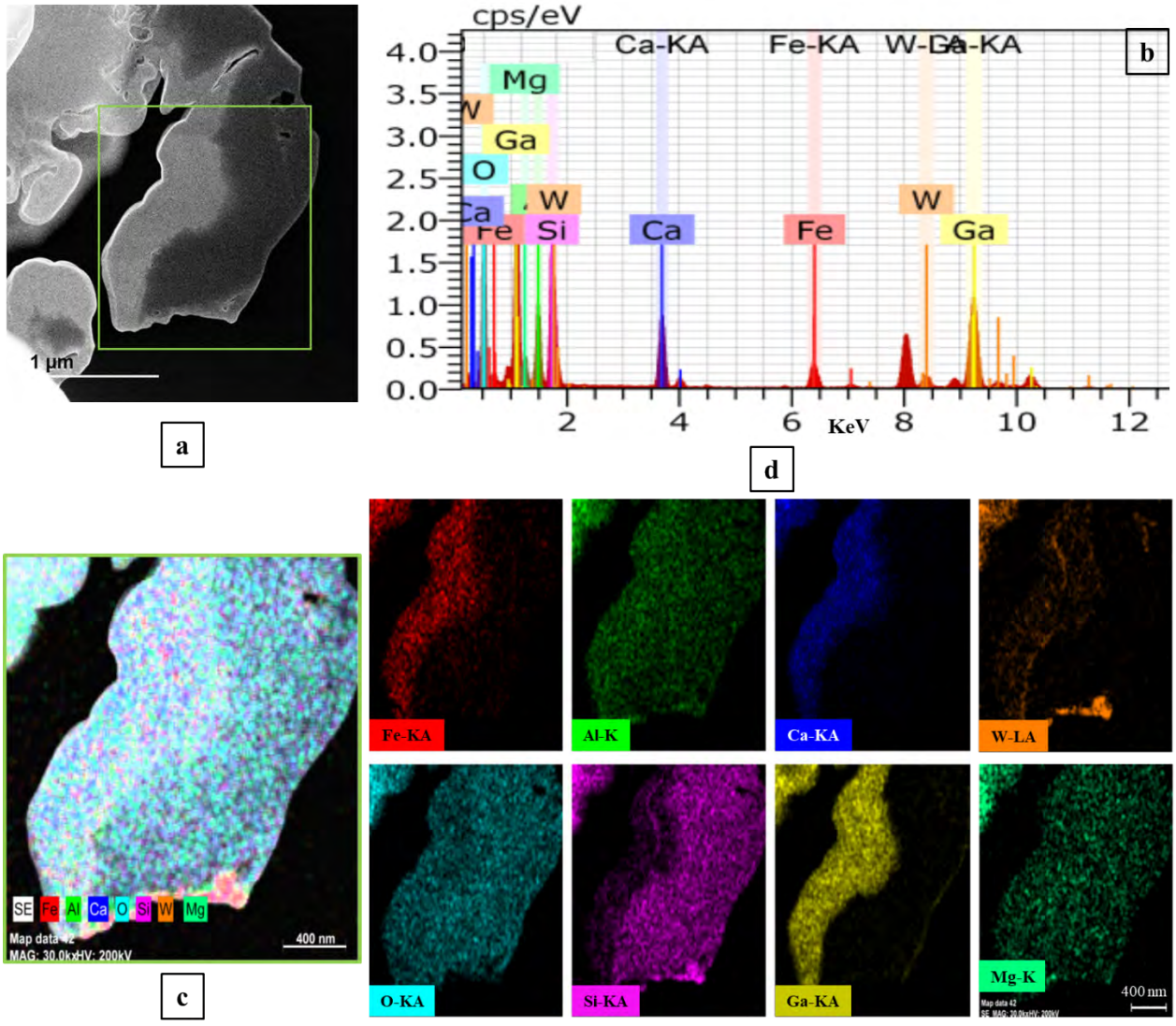

Figure 12: *EDS analysis and elemental mapping of CRM particle*

4 Conclusion

Through this study, a cementitious repair material has been fabricated by FIB system and studied analytically by STEHM. No previous studies documenting the nanostructure of this material when studied using STEHM (one of the highest resolution in the world) have been reported. After activating the CRM by water-spray, lift-out technique has been used in FIB system to manufacture appropriate size specimen (50~100 nm thickness) for STEHM analyses. Hydrated specimen revealed fine, compact, homogenous morphology and its diffraction pattern after water-activation indicated nearly amorphous structure, however, evidence of short-range structural was observed which requires further investigation. The relative thickness map, attained from hydrated particle under STEHM, indicated that measured specimen thickness, thinned through FIB processing, was about 40-70 nm which allows sufficient electrons to transfer inside sample. This preliminary investigation leaves many questions unanswered but demonstrates the feasibility of a powerful technique for examining the nanostructure of the cement-based material, and the effects of

its microstructure and solution compositions on the stage of hydration. Great care should be exercised when manipulating ion-thinned specimens in the STEHM because it is quite possible for an operator to be unaware about the damage that has occurred. This report provides new insights in the fabrication and examination of the microstructural development of cement-based products at the nano-scale.

5 Acknowledgement

Thanks are due to the Natural Sciences and Engineering Research Council of Canada (NSERC) for financial support. The authors are grateful to Drs. Rodney Herring, Elaine Humphrey, Arthur Buckham, and Mana Norouzpour for first engaging their interest in the subject of cement, and for continued valuable discussion.

6 Conflict of interest

The authors declare that there is no conflict of interest regarding the publication of this paper.

7 References

Borchert, H., Shevchenko, E.V., Robert, A., Mekis, I., Kornowski, A., Grübel, G., and Weller, H. (2005). Determination of Nanocrystal Sizes: A Comparison of TEM, SAXS, and XRD Studies of Highly Monodisperse CoPt3 Particles. Langmuir *21*, 1931–1936.

Card, J.A., Mohan, K., Taylor, H.F.W., and Cliff, G. (1980). Analytical Electron Microscopy of Cement Pastes: I, Tricalcium Silicate Pastes. Journal of the American Ceramic Society *63*, 336–337.

Chaunsali, P., and Peethamparan, S. (2013). Influence of the composition of cement kiln dust on its interaction with fly ash and slag. Cement and Concrete Research *54*, 106–113.

Ciach, T.D., Gillott, J.E., Swenson, E.G., and Sereda, P.J. (1971). Microstructure of calcium silicate hydrates. Cement and Concrete Research *1*, 13–25.

Crewe, A.V., Isaacson, M., and Johnson, D. (1969). A Simple Scanning Electron Microscope. Review of Scientific Instruments *40*, 241–246.

Crewe, A.V., Wall, J., and Langmore, J. (1970). Visibility of Single Atoms. Science *168*, 1338–1340.

Dalgleish, B.J., and Ibe, K. (1981). Thin-foil studies of hydrated Portland cement. Cement and Concrete Research *11*, 729–739.

Dalgleish, B.J., Pratt, P.L., and Moss, R.I. (1980). Preparation techniques and the microscopical examination of portland cement paste and C3S. Cement and Concrete Research *10*, 665–676.

Double, D.D., Hellawell, A., and Perry, S.J. (1978). The Hydration of Portland Cement. Proceedings of the Royal Society A: Mathematical, Physical and Engineering Sciences *359*, 435–451.

Ersoy, B., Dikmen, S., Uygunoğlu, T., İçduygu, M.G., Kavas, T., and Olgun, A. (2013). Effect of mixing water types on the time-dependent zeta potential of Portland cement paste. Science and Engineering of Composite Materials *20*.

Gallucci, E., Mathur, P., and Scrivener, K. (2010). Microstructural development of early age hydration shells around cement grains. Cement and Concrete Research *40*, 4–13.

Giannuzzi, L.A., and Stevie, F.A. (1999). A review of focused ion beam milling techniques for TEM specimen preparation. Micron *30*, 197–204.

Giannuzzi, L.A., Kempshall, B.W., Schwarz, S.M., Lomness, J.K., Prenitzer, B.I., and Stevie, F.A. (2005). FIB Lift-Out Specimen Preparation Techniques. In Introduction to Focused Ion Beams: Instrumentation, Theory, Techniques and Practice, L.A. Giannuzzi, and F.A. Stevie, eds. (Boston, MA: Springer US), pp. 201–228.

Groves, G.W. (1986). TEM Studies of Cement Hydration. MRS Proceedings *85*.

Groves, G.W., and Rodger, S.A. (1989). The hydration of C3S and ordinary Portland cement with relatively large additions of microsilica. Advances in Cement Research *2*, 135–140.

Groves, G.W., Le Sueur, P.J., and Sinclair, W. (1986). Transmission Electron Microscopy and Microanalytical Studies of Ion-Beam-Thinned Sections of Tricalcium Silicate Paste. Journal of the American Ceramic Society *69*, 353–356.

Grudemo, A. (1964). The Chemistry of Cements (New York: Academic Press).

Grutzeck, M.W., and Roy, D.M. (1969). Electron Microprobe Studies of the Hydration of 3CaO.SiO2. Nature *223*, 492–494.

Henderson, E., and Bailey, J.E. (1988). Sheet-like structure of calcium silicate hydrates. Journal of Materials Science *23*, 501–508.

Hou, P., Cheng, X., Qian, J., Zhang, R., Cao, W., and Shah, S.P. (2015). Characteristics of surface-treatment of nano-SiO2 on the transport properties of hardened cement pastes with different water-to-cement ratios. Cement and Concrete Composites *55*, 26–33.

Javelas, R., Maso, J.C., and Ollivier, J.P. (1974). Realisation de lames ultra-minces de mortier pour observation directe au microscope electronique par transmission. Cement and Concrete Research *4*, 167–168.

Jennings, H.M., and Pratt, P.L. (1980). The Use of a High Voltage Electron Microscope and Gas Reaction Cell for the Microstructural Investigation of Wet Portland Cement. Journal of Materials Science Letters 250–253.

Jennings, H.M., Dalgleish, B.J., and Pratt, P.L. (1981). Morphological Development of Hydrating Tricalcium Silicate as Examined by Electron Microscopy Techniques. Journal of the American Ceramic Society *64*, 567–572.

Kumar, M., Singh, N.P., and Singh, N.B. (2009). Effect of water proofing admixture on the hydration of Portland cement. Indian Journal of Chemical Technology *16*, 499–506.

Lachowski, E.E., and Diamond, S. (1983). Investigation of the composition and morphology of individual particles of portland cement paste: 1. C-S-H gel and calcium hydroxide particles. Cement and Concrete Research *13*, 177–185.

Lachowski, E.E., Mohan, K., Taylor, H.F.W., and Moore, A.E. (1980). Analytical Electron Microscopy of Cement Pastes: II, Pastes of Portland Cements and Clinkers. Journal of the American Ceramic Society *63*, 447–452.

Lachowski, E.E., Mohan, K., Taylor, H.F.W., Larsen, C.D., and Moore, A.E. (1981). Analytical Electron Microscopy of Cement Pastes: III, Pastes Hydrated for Long Times. Journal of the American Ceramic Society *64*, 319–321.

Lin, K.L., Chang, W.C., Lin, D.F., Luo, H.L., and Tsai, M.C. (2008). Effects of nano-SiO2 and different ash particle sizes on sludge ash–cement mortar. Journal of Environmental Management *88*, 708–714.

Plank, J., Dai, Z., and Andres, P.R. (2006). Preparation and characterization of new Ca–Al–polycarboxylate layered double hydroxides. Materials Letters *60*, 3614–3617.

Ramezanianpour, A.A., Ghahari, S.A., and Esmaeili, M. (2014). Effect of combined carbonation and chloride ion ingress by an accelerated test method on microscopic and mechanical properties of concrete. Construction and Building Materials *58*, 138–146.

Richardson, I.G. (1999). The nature of C-S-H in hardened cements. Cement and Concrete Research *29*, 1131–1147.

Richardson, I.G. (2002). Electron microscopy of cements. In Structure and Performance of Cements, (London; New York: Spon Press), p.

Richardson, I.G. (2004). Tobermorite/jennite- and tobermorite/calcium hydroxide-based models for the structure of C-S-H: applicability to hardened pastes of tricalcium silicate, β-dicalcium silicate, Portland cement, and blends of Portland cement with blast-furnace slag, metakaolin, or silica fume. Cement and Concrete Research *34*, 1733–1777.

Richardson, I.G., and Groves, G.W. (1992). Microstructure and microanalysis of hardened cement pastes involving ground granulated blast-furnace slag. Journal of Materials Science *27*, 6204–6212.

Richardson, I.G., and Groves, G.W. (1993). Microstructure and microanalysis of hardened ordinary Portland cement pastes. Journal of Materials Science *28*, 265–277.

Rodger, S.A., and Groves, G.W. (1989). Electron Microscopy Study of Ordinary Portland Cement and Ordinary Portland Cement–Pulverized Fuel Ash Blended Pastes. Journal of the American Ceramic Society *72*, 1037–1039.

Scrivener, K.L. (1984). The development of microstructure during the hydration of Portland cement. PhD thesis. University of London.

Scrivener, K.L., and Pratt, P. (1984). Microstructural studies of the hydration of C3A and C4AF independently and in cement paste. pp. 207–219.

Scrivener, K.L., and Pratt, P.L. (1983). Characterisation of Portland Cement Hydration by Electron Optical Techniques. MRS Proceedings *31*.

Sharif, A. (2016). Review on advances in nanoscale microscopy in cement research. Micron *80*, 45–58.

Sisomphon, K., Copuroglu, O., and Koenders, E.A.B. (2012). Self-healing of surface cracks in mortars with expansive additive and crystalline additive. Cement and Concrete Composites *34*, 566–574.

Sun, Y., Zhang, Z., and Wong, C.P. (2005). Study on mono-dispersed nano-size silica by surface modification for underfill applications. Journal of Colloid and Interface Science *292*, 436–444.

Taylor, H.F. (1997). Cement chemistry (Thomas Telford).

Taylor, H.F.W., Mohan, K., and Moir, G.K. (1985). Analytical Study of Pure and Extended Portland Cement Pastes: I, Pure Portland Cement Pastes. Journal of the American Ceramic Society *68*, 680–685.

Tiegs, T.N. (1975). Investigation of Ion Thinned Tricalcium Silicate Pastes by Transmission Electron Microscopy. M. Sc. Thesis. University of Illinois.

Viehland, D., Li, J.-F., Yuan, L.-J., and Xu, Z. (1996). Mesostructure of Calcium Silicate Hydrate (C-S-H) Gels in Portland Cement Paste: Short-Range Ordering, Nanocrystallinity, and Local Compositional Order. Journal of the American Ceramic Society *79*, 1731–1744.

Xin, H.L., Niu, K., Alsem, D.H., and Zheng, H. (2013). In Situ TEM Study of Catalytic Nanoparticle Reactions in Atmospheric Pressure Gas Environment. Microscopy and Microanalysis *19*, 1558–1568.

Zhang, F., Jin, Q., and Chan, S.-W. (2004). Ceria nanoparticles: Size, size distribution, and shape. Journal of Applied Physics *95*, 4319–4326.

Ziel, R., Haus, A., and Tulke, A. (2008). Quantification of the pore size distribution (porosity profiles) in microfiltration membranes by SEM, TEM and computer image analysis. Journal of Membrane Science *323*, 241–246.